Multi-service Routing with Guaranteed Load Balancing for LEO Satellite Networks

Cui-Qin Dai[1(✉)], Guangyan Liao[1], P. Takis Mathiopoulos[2], and Qianbin Chen[3]

[1] School of Communication and Information Engineering, Chongqing University of Posts and Telecommunications, Chongqing, China
daicq@cqupt.edu.cn, liaogy.cqupt@qq.com

[2] Department of Informatics and Telecommunications, National and Kapodestrian University of Athens, Athens, Greece
mathio@di.uoa.gr

[3] Chongqing Key Lab of Mobile Communication Technology, Chongqing University of Posts and Telecommunications, Chongqing, China
chenqb@cqupt.edu.cn

Abstract. Low Earth Orbit (LEO) Satellite Networks (SN) offers communication services with low delay, low overhead, and flexible networking. As service types and traffic demands increase, the multi-service routing algorithms play an important role in ensuring users' Quality of Service (QoS) requirements in LEO-SN. However, the multi-service routing algorithm only considers the link QoS information, ignoring the uneven distribution of ground users, causing satellite link or node congestion, increasing the packet transmission delay, and packet loss rate. In order to solve the above problems, we propose a Multi-Service Routing with Guaranteed Load Balancing (MSR-GLB) algorithm which balances the network load while satisfying multi-service QoS requirements. Firstly, the Geographic Location Information Factors (GLIF) are defined to balance the network load by scheduling the ISLs with lower loads. Then, the optimization objective function is constructed by considering delay, remaining bandwidth, packet loss rate, and GLIF in order to characterize the routing problems caused by multi-service and load balancing. Following this, we propose an MSR-GLB algorithm that includes the state transition rule and the pheromone update rule. Among them, the state transition rule is based on QoS information and link GLIF, and the pheromone update rule has the characteristics of positive and negative feedback mechanism. The simulation results show that the MSR-GLB algorithm can well meet the QoS requirements of different services, balance the network load compared to Cross-layer design and Ant-colony optimization based Load-balancing routing algorithm in LEO Satellite Network (CAL-LSN) and Multi-service On-demand Routing (MOR) algorithm.

Keywords: LEO satellite network · Routing · Multi-service · Load balancing

1 Introduction

As an indispensable part of future communications, Low Earth Orbit Satellite Networks (LEO-SN) offer high-speed and reliable data transmission with wider coverage, higher

H. Gao et al. (Eds.): ChinaCom 2019, LNICST 312, pp. 283–298, 2020.
https://doi.org/10.1007/978-3-030-41114-5_22

bandwidth, lower delay, and cost-efficient networking capabilities [1]. As the capacity of Inter-Satellite Links (ISLs) increases coupled with the great enhancement of on-board signal processing capabilities of LEO-SN, routing plays an important role to fulfil the requirements of high-speed, low-delay and reliable transmission for spatial information [2].

For dynamic SN, the traditional routing algorithms can be broadly divided in accordance to the topology control methods as follows: (i) Virtual topology routing [3]; (ii) Virtual node routing [4]; and (iii) Footprint-based routing [5]. Among these three categories, virtual topology routing has become more popular as it requires lower on-board processing capability and supports wider orbit type characteristics, e.g. see [6, 7]. The algorithms described in [6, 7] deal with the Quality of Service (QoS) of a single service and have proposed optimal routing paths. However, the LEO-SCN service types have been diversified because of its rapid development, and the different service types require different QoS requirements. In a consequence, various optimization researches for multi-service routing algorithms have been published in the past, including [8–11]. In [8], a Multi-service On-demand Routing (MOR) protocol, which adopts different routing modes for different service types to improve network efficiency while ensuring different service QoS, has been proposed. In [9, 10], the services were classified according to the QoS requirements of various services, and then corresponding routing algorithms are designed for different services. In order to solve the problem of service quality requirements for different services and unbalanced link resource utilization, a multi-service routing algorithm based on multi-objective decision-making for LEO satellite network was proposed in [11]. However, under high traffic loads, some ISLs in these algorithms may become heavily loaded even congested while others remain in underutilized condition.

Another commonly encountered problem with LEO-SN is that of Load Balancing (LB) which typically occurs because of the uneven distribution of ground users. In the past there have been several attempts to include the LB into the design of the routing algorithms, e.g. see [12–14]. For example, Song et al. in [12] have proposed a Traffic-Light-based intelligent Routing strategy (TLR). A Cross-layer design and Ant-colony optimization based Load-balancing routing algorithm in LEO Satellite Network (CAL-LSN), which uses multi-objective optimization model to achieve load balancing, and can meet the requirement of video transmission, was introduced in [13]. In [14], a hybrid global-local load routing scheme was proposed by taking advantage of the predictive nature of Internet of Things (IoT) traffic distribution as well as the position of the LEO satellites. It should be emphasized that all these load balancing routing algorithms are designed to optimize the QoS of a single service, i.e. they don't consider the fact that different services usually have different QoS requirements.

From the previous literature review, it is evident that no generic approach exists which can deal effectively with multi-service and load-balancing routing problems encountered in LEO-SCN supporting multiple services and high traffic. In order to fill this gap, in this paper, we address such problems by providing a solution to the following question: How should the network load be balanced while satisfying multi-service QoS requirements in LEO-SCN? In particular, a Multi-Service Routing with Guaranteed Load Balancing (MSR-GLB) algorithm was proposed by taking into account the influence of factors

such as delay, residual bandwidth, packet loss rate and geographic location information factor (GLIF) on path selection. Firstly, the GLIF was defined by analyzing the traffic demand distributions of satellites covering terrestrial users to show the relative traffic load of the ISLs. Secondly, the routing problem is formulated as a multi-constrained QoS optimization objective function by considering link QoS information and GLIF. Finally, the state transition rule was improved to obtain an optimal transmission path that satisfies the QoS requirements of different services and balances the network load, and the pheromone updating rule was optimized by positive feedback and negative feedback mechanism.

The remainder of this paper is organized as follows. Section 2 presents the system model, which is composed of the system network model and GLIF. Section 3 introduces problem formulation. Section 4 introduces the MSR-GLB algorithm proposed in this paper. This is following by the performance evaluation results and discussion in Sect. 5. And Sect. 6 concludes this paper.

2 System Model

In this section, the satellite network model will be first presented. Then, we have defined GLIF. The load status of the inter-satellite link is predicted by the value of GLIF.

2.1 Satellite Network

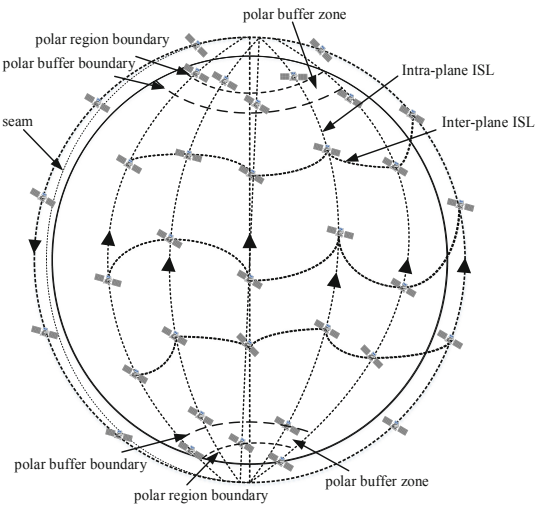

Fig. 1. The considered Iridium-like LEO satellite network constellation.

As illustrated in Fig. 1, we consider a LEO Iridium-like constellation, which consists of six planes with an inclination of having 11 satellites distributed in every plane [15]. For the operation of this satellite network, each satellite has four ISLs: two IntrA-Plane (IAP)

ISLs and two IntEr-Plane (IEP) ISLs, expect for the satellites along the counter-rotating seam only have three active ISLs, because the cross-seam ISLs, namely links between satellites in counter-rotating orbits, are not used due to link acquisition and special antenna steering requirement. The IAP ISLs connect adjacent satellites within the same plane, while IEP ISLs link connects adjacent satellites across neighboring orbits. The IAP ISLs is maintained all times as the same orbital operation rule is followed and the nodes are relatively stationary, and is expressed as Eq. (1).

$$L_{\mathrm{a}} = \sqrt{2}R\sqrt{1 - \cos(\frac{2\pi}{M})} \tag{1}$$

where M is the number of satellites each plane and R is the radius of the earth.

The IEP ISLs lengths vary over time with the satellite movement, and the on-off state switching of IEP links is carried out because the satellite trajectory operates differently. When the satellite moves toward the Polar Regions, the IEP ISLs become shorter, as in Eq. (2).

$$L_{\mathrm{e}} = \sqrt{2}R\sqrt{1 - \cos(2\pi\frac{1}{2N})}\cos(\mathrm{lat}) \tag{2}$$

where N is the number of planes and lat represents for the latitude difference at which the IEP ISLs.

The high-speed motion of the satellite network has resulted in the change of the network topology, but it has periodicity and predictability. In a certain time range, it considered that the network topology is fixed. For the LEO satellite network, the virtual topology strategy [16] makes the entire topology in a relatively static state, namely, a complete satellite system operation cycle T divided into n definite time slice, it is $[t_0 = 0, t_1], [t_1, t_2], \cdots, \left[t_{n-1}, t_n = T\right]$. And each time segment has the following characteristics: The network topology is invariable, and the network topology changes and link switching occurs only at time point $t_0, t_1, \cdots, t_n$.

2.2 Geographic Location Information Factor

Due to the differences in geography, climate and economic development, the population distribution is relatively uneven, so the number of users accessing the satellite network varies. According to the level of traffic load, the satellite coverage surface is divided into hotspot and non-hotspot zones [17]. According to the distribution of the world population and their telecommunication needs, three hotspots were set up, namely Eastern Asia, North America, Europe-Western Asia. Figure 2 depicts the division strategy of these hotspot zones while Table 1 presents their central latitudes. In order to avoid satellite network congestion, the traffic can be actively dispersed, that is, the traffic of high-load ISLs is dispersed to low-load ISLs for transmission. Consequently, we can define the Geographic Location Information Factor (GLIF) to estimate the ISLs load status. The GLIF can be expressed as a function related to the geographic location of the satellite. The higher the GLIF value is, the traffic load on the satellite inter-satellite link is greater. Following the type of satellite links, the GLIF is divided into IAP-GLIF and IEP-GLIF. The relevant equation is shown in Eqs. (3) and (4).

(1) IntrA-Plane Geographic Location Information Factor (IAP-GLIF)

$$\lambda_{\text{u-intra}} = \begin{cases} \exp\left(2lat_u / \pi\right), -\pi / 2 \le lat_u \le lat_c \\ \exp\left(-2(lat_u - 2lat_c) / \pi\right), lat_c \le lat_u \le \pi / 2 \end{cases} \tag{3}$$

where lat_u denotes the latitude of the satellite node u. Here, $lat_c (0 < lat_c < \pi / 2)$ denotes the latitude of the central area of hotspot zones within the Northern Hemisphere. Hereinafter, lat_c is called as central latitude.

(2) IntEr-Plane Geographic Location Information Factor (IEP-GLIF)

$$\lambda_{\text{u-inter}} = \begin{cases} \exp\left(-2(lat_u + 2lat_T) / \pi\right), -\pi / 2 \le lat_u < -lat_T \\ \exp\left(lat_u / \pi\right), -lat_T \le lat_u < lat_c \\ \exp\left(-2(lat_u - 2lat_c) / \pi\right), lat_c \le lat_u < lat_T \\ \exp\left(2(lat_u + 2lat_c - 2lat_T) / \pi\right), lat_T \le lat_u \le \pi / 2 \end{cases} \tag{4}$$

where lat_T denotes the threshold latitude.

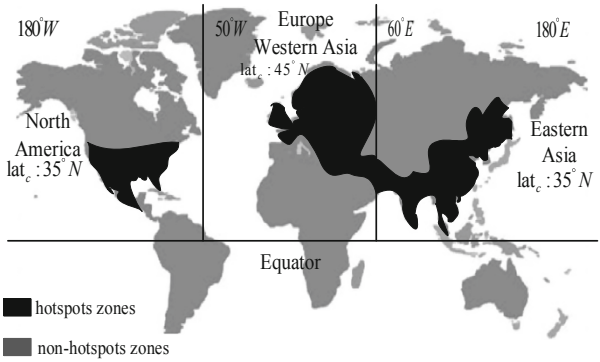

Fig. 2. Division of hotspot zones.

Table 1. Parameters for the division.

Name	Coverage area	Central latitude
Eastern Asia	$60^\circ E$–$180^\circ E$	$35^\circ N$
North America	$50^\circ W$–$180^\circ W$	$35^\circ N$
Europe-Western Asia	$50^\circ W$–$60^\circ E$	$45^\circ N$

3 Problem Formulation

With the rapid development of LEO satellite networks, the types of services are also developing and changing differently day by day. According to the QoS requirements of

diverse services such as data, voice and video, the services are divided into three types [18]: Class A is the delay-sensitive service, such as command voice with high latency requirements; Class B is the bandwidth-sensitive service, such as the terrestrial observing service. Class C is the packet loss rate of sensitive service. The packet transmission of their path requires low latency, high residual bandwidth, and low packet loss rate, respectively.

When the satellite nodes in the network are moving in its orbit, the service types are changing accordingly. However, the different service types have different requirements for QoS, and the optimization for a certain QoS parameter cannot satisfy the user's needs. Meanwhile, due to the rapid growth of satellite communication service demand and the uneven distribution of satellite coverage services demand on the ground, the path of routing calculation is easy to select the link of the hotspot zones, which leads to link and node congestion. Therefore, in order to meet the diversified service requirements and balance the network load, the optimization function is proposed, as in Eq. (5).

$$\begin{aligned} &\min \mathrm{F} = \sum_{e(i,j)\in p_{SD}} \lambda_{ij}\left(\mathrm{w}_1\left(d_{ij}/D\max\right) + \mathrm{w}_2\left(C\min/c_{ij}\right) + \mathrm{w}_3\left(l_{ij}/L\max\right)\right) \\ &s.t.\quad d_{P_{SD}} = \sum_{e(i,j)\in p_{SD}} d_{ij} \le D\max \\ &\quad c_{P_{SD}} = \min_{e(i,j)\in p_{SD}} \left\{c_{ij}\right\} \ge C\min \\ &\quad l_{P_{SD}} = \left(1 - \prod_{e(i,j)\in p_{SD}} (1 - l_{ij})\right) \le L\max \end{aligned} \tag{5}$$

where $\lambda_{ij}(t)$ represents the GLIF of link $e(i, j)$; P_{SD} represents the path from the source satellite S to the destination satellite D; $e(i, j)$ is the link between satellite nodes i and j; d_{ij} represents the delay of the link $e(i, j)$; c_{ij} denotes the remaining bandwidth of the link $e(i, j)$; l_{ij} is the packet loss rate of the link $e(i, j)$ and $\mathrm{w}_k \in [0, 1](k = 1, 2, 3)$ is the weighting factors of the link QoS attribute, i.e., the delay, residual bandwidth, and packet loss rate, for the link $e(i, j)$, which can be evaluated by the eigenvector method [11]. $d_{P_{SD}}$, $c_{P_{SD}}$, and $l_{P_{SD}}$ represent the delay, remaining bandwidth, and packet loss rate of the path P_{SD}, respectively. $D_{\max}$, $C_{\min}$, and $L_{\max}$ represent the QoS attribute constraint values of the ideal path P_{SD} such as delay, residual bandwidth, and packet loss rate, respectively. The relevant QoS attribute definitions are as follows:

Delay: It is the sum of the propagation delay and queuing delay of the data packet, and is expressed as Eq. (6).

$$d_{ij} = d_p(i, j) + d_q(i, j) \tag{6}$$

where, $d_p(i, j)$ and $d_q(i, j)$ are the propagation delay and queuing delay of the link $e(i, j)$. The relevant equation is shown in Eqs. (7) and (8).

$$d_p(i, j) = \frac{L(i, j)}{c_p} \tag{7}$$

where $L(i, j)$ is the length of the inter-satellite link $e(i, j)$, and c_p is the speed of light.

$$d_q(i, j) = \frac{N_q(i, j) \times L_\alpha}{C} \tag{8}$$

where $N_q(i, j)$ is the number of packets in the buffer of $e(i, j)$. L_α is the average length of packets. C is the total link capacity of the link.

The delay is the additive parameter, that is, the total delay of the path P_{SD} is equal to the sum of the delay of each link in the path P_{SD}.

Remaining bandwidth: The remaining bandwidth is the total bandwidth of the link minus the link bandwidth used by the transport packet. As shown in Eq. (9).

$$c_{ij} = C - c_{used}(i, j) \tag{9}$$

where C is the total link capacity of the link $e(i, j)$. $c_{used}(i, j)$ is the bandwidth used by the link $e(i, j)$.

The remaining bandwidth is a concave parameter, where the remaining bandwidth of each link in the path P_{SD} is compared, and the minimum value is taken as the residual bandwidth value of the path P_{SD}.

Packet loss rate: The packet loss rate is the ratio of the number of lost packets to the all transmitted data packets per unit time. It is a multiplicative parameter, and is expressed as Eq. (10).

$$l_{ij} = \frac{N_{\text{lost}}(i, j)}{N_{all\_send}(i, j)} \tag{10}$$

where, $N_{\text{lost}}(i, j)$ is the lost packet in link $e(i, j)$ and $N_{all\_send}(i, j)$ is the total data packet sent by link $e(i, j)$ per unit time.

4 The MSR-GLB Algorithm

In this section, we firstly introduce the MSR-GLB algorithm, and then introduce two important processes in the MSR-GLB algorithm, namely state transition rules and pheromone update rules. To solve this problem, we introduced an Ant Colony Optimization (ACO)[1]. In the pathfinding process, they behave very similarly, that is, the satellite node selects the path according to the link QoS information and GLIF, and the ants select the path according to the link pheromone. In addition, ACO has the characteristics of positive feedback mechanism, strong robustness, distributed computing and low complexity, which can find a better solution for solving multi-constrained optimization problems [20, 21]. Therefore, it is feasible to apply the ACO algorithm to the satellite network to solve the multi-service problem and load problem in this paper.

4.1 Algorithm Presentation

The MSR-GLB algorithm is an intelligent bionic algorithm based on ACO. In the pathfinding process, the MSR-GLB performs the next hop node selection depending on

[1] The ACO algorithm was proposed by the famous Italian scholar Dorigo [19] in 1991. The algorithm simulates that ants will leave a pheromone on the path when they are foraging. The concentration of the pheromone is inversely proportional to the path length and will volatilize as time passed. More specifically, the shorter path owns such more pheromone that it attracts a larger number of ants going along itself. After a period, the shortest path will always be selected.

the link pheromone, QoS status information, and GLIF. In addition, MSR-GLB updates the pheromone of the link through positive and negative feedback mechanisms, so that the ant colony quickly converges the optimal path. When the source satellite S makes a routing request of sending a message to the destination satellite D, the corresponding MSR-GLB algorithm steps are listed in the following. The MSR-GLB algorithm flow chart is shown in Fig. 3. We also have the corresponding pseudo-code in Algorithm 1.

Step 1: The satellite network topology $G(V, E)^t$ is obtained under the determined current satellite cycle time slot t and then the searching is started based on the network topology.

Step 2: Determine the type of service and initialize the network parameters: QoS parameters of links in the network, limit values of multi-constraint QoS conditions, initial pheromone concentration $\tau(0)$, volatilization coefficient ρ, pheromone factor α, QoS status factor β, GLIF factor r, pheromone punishment coefficient c, ant number m, maximum cycle number $NC_{\max}$, etc.

Step 3: Obtaining any pair of source-destination node pairs (S, D), and setting the number of cycles nc to 0.

Step 4: The ant searches for the path from the source node S.

Step 5: Initialize and update the current node: The source node initializes the current node and the next hop node updates the current node, and the current node is added to the tabu table.

Step 6: The ant determines whether the $allowed$ of the current node is empty or not. If it is empty, the pathfinding fails and process to step 9. Otherwise, it executes the next step.

Step 7: The ant selects the next hop node according to the state transition rule (11), and adds the selected node to the tabu table.

Step 8: The ant judges whether the next hop node is the destination node or not and if it is destination node then the path search succeeds and process to step 9, otherwise it returns to step 5.

Step 9: Whether all ants complete the pathfinding. If it is fulfilled, the pheromone is updated according to the pheromone updating rule (13) and the number of cycles is $nc = nc + 1$, otherwise goes back to the step 4.

Step 10: If the nc reaches to the maximum number of cycles $NC_{\max}$, the output is the optimal solution of the corresponding transmission path otherwise it goes back to the step 4.

Algorithm 1 MSR-GLB algorithm

Input: The network topology $G(V,E)^t$, the number of satellite nodes n, the type of service, the limit values of multi-constraint QoS conditions, initial pheromone concentration $\tau(0)$, volatilization coef cient ρ, pheromone factor α, QoS status factor β, GLIF factor r, pheromone punishment coef cient c, ant number m, maximum cycle number NC_{max}, source node S, destination node D.

Output: The best solution corresponding to the transmission path

Initialization: $currentnode = S$, $cyclenumber = 1$,
for $i = 1,2,...,n$ **do**
    Set $allowed(i) = 1$
end for
while $cyclenumber <= NC_{max}$ **do**
    for $i = 1,2,...,m$ **do**
        while $currentnode \neq D$ **do**
            for each node j in the neighbor list of current node **do**
                if $allowed(j) == 1$ **then**
                    Choose the next hop x with the state transition rule
                    Set $allowed(x) = 0$
                end if
            end for
            $currentnode = x$
        end while
    end for
    for each link **do**
        Update the pheromone value
    end for
end while

4.2 State Transition Rule

When the ant k reaches the satellite node i, the next hop satellite node j is selected according to the pseudo-random scale rule. The next hop node selection rule is expressed as Eq. (11).

$$\mathrm{j} = \begin{cases} \arg \max\limits_{j \in allowed_k} \left\{ \tau_{ij}^{\alpha}(t) \eta_{ij}^{\beta}(\mathrm{t}) \xi_{ij}^{r}(t) \right\}, & q \leq q_0 \\ \mathrm{J} \quad , & q > q_0 \end{cases} \tag{11}$$

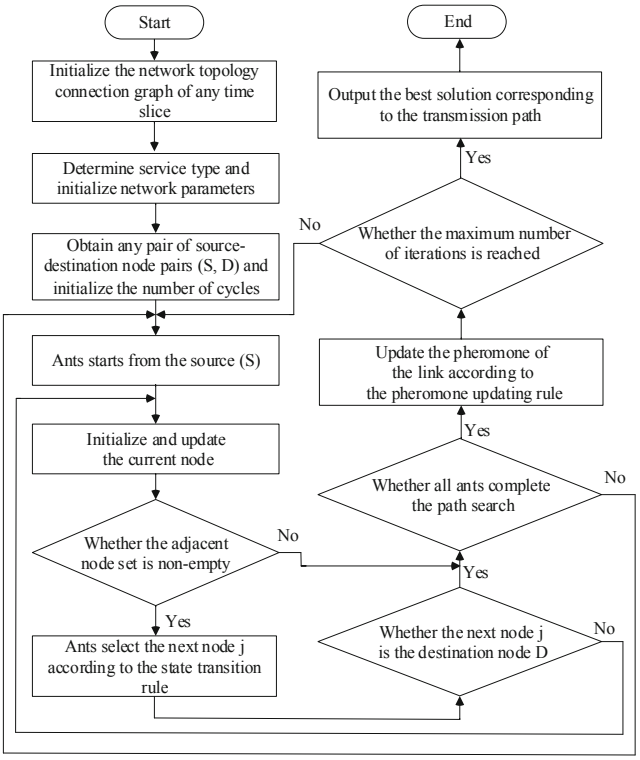

Fig. 3. Flow chart of MSR-GLB algorithm.

where $allowed_k = \{V(i,:) - tabu_k\}$ represents the set of satellite nodes that the ant k next hop can select, and the ant adds the node to the tabu table $tabu_k$ every time a node passes. $\tau_{ij}(t)$ represents the pheromone concentration of the link $e(i, j)$ at time t, and will be over time volatile. $\eta_{ij}(t) = 1/\omega_{ij}(t)$, $\omega_{ij}(t) = w_1(d_{ij}/D_{max}) + w_2(C_{min}/c_{ij}) + w_3(l_{ij}/L_{max})$ represents the QoS status value of the link $e(i, j)$ at time t. $\xi_{ij}(t) = 1/\lambda_{ij}(t)$. α, β, and r reflect the relative importance of pheromones concentration, QoS status value, and GLIF of the link $e(i, j)$ during the path finding process. $q \sim U(0, 1)$, and $q_0 \in [0, 1]$ is a parameter which determines the relative importance of exploitation versus exploration: the ant k samples a random number $0 \leq q \leq 1$. If $q \leq q_0$ then the best next hop node, according to (11) is chosen, otherwise a next hop node is chosen according to (12). J is a random variable selected according to the probability distribution, as in Eq. (12).

$$p_{ij}^k(t) = \begin{cases} \dfrac{\tau_{ij}^{\alpha}(t)\eta_{ij}^{\beta}(t)\xi_{ij}^{r}(t)}{\sum\limits_{s \in allowed_k} \tau_{is}^{\alpha}(t)\eta_{is}^{\beta}(t)\xi_{is}^{r}(t)}, & j \in allowed_k \\ 0, & \text{elsewhere} \end{cases} \tag{12}$$

4.3 Pheromone Updating Rule

After completing one iteration, all ants have used positive and negative feedback mechanisms to update the pheromone on the path. The pheromone concentration on the corresponding link increases when the ant finds the path successfully, otherwise the concentration decreases. The pheromone updating rule is expressed as Eq. (13).

$$\tau_{ij}(t+1) = (1-\rho)\tau_{ij}(t) + \Delta\tau_{ij}^{s}(t) + \Delta\tau_{ij}^{f}(t) \tag{13}$$

where $\rho \in (0, 1)$ is the pheromone volatilization coefficient. $\Delta\tau_{ij}^{s}(t)$ represents the pheromone increment on the link $e(i, j)$ of all ants reaching the destination node success at time t, $\Delta\tau_{ij}^{f}(t)$ represents the pheromone reduction on the link $e(i, j)$ of all ants reaching the destination node failure at time t. The relevant equation is shown in Eqs. (14), (15), (16) and (17).

$$\Delta\tau_{ij}^{s}(t) = \sum_{\mathrm{k}=1}^{m} a_{ij}^{k}\eta_{ij}^{k}(t)\xi_{ij}^{k}(t) + a_{ij}^{M}\eta_{ij}^{M}(t)\xi_{ij}^{M}(t)\,, ij \in path \tag{14}$$

$$a_{ij}^{k} = \begin{cases} 1, (flag == success \,\&\&\, ij \in path^{k}) \\ 0, (flag == failure \,\&\&\, ij \in path^{k}) \end{cases} \tag{15}$$

where $path$ represents the path set of all ants, i.e. $path = \left\{path^{1}, path^{2}, \cdots, path^{m}\right\}$. a_{ij}^{k} indicates whether ant k increases the link $e(i, j)$ pheromone concentration. M is the ant corresponding to the minimum QoS status value of the current iteration. $\sum_{ij \in path} \omega_{ij}^{nc,k}$ is the QoS status value of the current iteration ant k. $flag$ indicates whether the ant k has successfully reached the destination node. If it reaches the destination node successfully, the value of $flag$ is $success$; otherwise, it is $failure$.

$$\Delta\tau_{ij}^{f}(t) = \mathrm{c}\sum_{k=1}^{m} b_{ij}^{k}\eta_{ij}^{k}(t)\xi_{ij}^{k}(t)\,, ij \in path \tag{16}$$

$$\mathrm{b}_{ij}^{k} = \begin{cases} 0, (flag = success \,\&\&\, ij \in path^{k}) \\ -1, (flag = failure \,\&\&\, ij \in path^{k}) \end{cases} \tag{17}$$

where $c \in [0, 1]$ is the pheromone punishment coefficient, and b_{ij}^{k} indicates whether ant k decreases the pheromone concentration on the link $e(i, j)$.

5 Performance Evaluation Results and Discussion

5.1 Simulation Platform

An Iridium-like constellation system is built using the Satellite Tool Kit (STK). The specific parameters are shown in Table 2. Other simulation parameters are set to: number of ants $m = 40$, number of iterations $NC_{\max} = 50$, $\alpha = 2$, $\beta = 4$, $r = 2$, $\mathrm{c} = 0.1$,

$\rho = 0.3$, $\tau(0) = 50$, $q_0 = 0.1$, $lat_T = 70^{\circ}$, $lat_c = 45^{\circ}$. In the simulation, the inter-satellite link bandwidth is 10 Mbit/s, and each output Link is allocated a 4 MB buffer with an average packet size of 500 B. Five pairs of source-destination nodes are randomly selected; the simulation time is 100 min, and the number of node requests increases with time.

When the delay sensitive service, the bandwidth sensitive service, and the packet loss rate sensitive service are simultaneously present in the network, and the source node and the destination node are the same, the transmission efficiency of the three types of services is shown in Table 3. The relative importance of each QoS attribute calculated by the eigenvector method is shown in Table 4.

Table 2. Iridium-like constellation system parameter.

Parameters	Value
Orbit height	780 km
Number of orbital planes	6
Number of satellites in orbit	11
Track inclination	86.4°
Polar buffer boundary latitude	60°
Polar region boundary latitude Threshold	70°

Table 3. Service transmission efficiency parameters.

Services type	Delay (ms)	Average bandwidth (Mbit/s)	Packet loss rate (%)
Delay Sensitive Services	83.6	3	0.06
Bandwidth Sensitive Services	98.7	4	0.08
Packet Loss Rate Sensitive Services	91.2	2	0.03

Table 4. Relative importance.

Services type	Relative importance
Delay Sensitive Services	(0.55 0.24 0.21)
Bandwidth Sensitive Services	(0.25 0.54 0.21)
Packet Loss Rate Sensitive Services	(0.26 0.20 0.54)

5.2 Results and Analysis

The MSR-GLB algorithm is compared with CAL-LSN and MOR to evaluate network performance such as end-to-end delay, packet loss rate, throughput, and traffic distribution index.

As shown in Fig. 4, with the increase of simulation time, the end-to-end delay of MSR-GLB algorithm is lower than CAL-LSN and MOR. Because the CAL-LSN algorithm guarantees reliable transmission of data packets, selects the minimum hop path, and does not consider the delay. The MOR algorithm designs different routing algorithms for different services, considers the delay of the link for delay-sensitive and best-effort services, and considers the bandwidth and number of paths for the bandwidth-sensitive service. When the network load is aggravated, the algorithm is prone to link congestion, resulting in increased delay. The MSR-GLB algorithm considers the delay of the link for different services, and the delay has different weights in different services.

As shown in Fig. 5, as the simulation time increases, the packet loss rate of the three routing algorithms increases, but the packet loss rate of the MSR-GLB algorithm is lower than CAL-LSN and MOR. The CAL-LSN algorithm selects the link with a relatively small error rate when selecting the path, but does not support multiple QoS. Although the MOR algorithm designs different routing algorithms for different services, it does not consider the packet loss rate information of the link. However, when the MSR-GLB algorithm performs path selection for the service, regardless of the service, the packet loss information of the link is considered, and the path transmission of the lower packet loss information is selected.

As shown in Fig. 6, the throughput of the three algorithms increases with the simulation time increases, and the performance of the MSR-GLB algorithm throughput is advantageous. The CAL-LSN algorithm considers the remaining bandwidth of the link when selecting the path but does not consider the packet loss rate of the link. The MOR algorithm uses different routing algorithms for different service types, but does not consider the load state of the link. When the network load is large, MOR and CAL-LSN packet loss is more serious. Nevertheless, the MSR-GLB algorithm considers not only the remaining bandwidth of the link and the packet loss rate when selecting paths for different services but also the geographic location information factor of the network.

As shown in Fig. 7, as the simulation time increases, the traffic distribution index of the three algorithms increase, but the MSR-GLB algorithm is better than the other two algorithms. The CAL-LSN algorithm ensures reliable transmission of data packets and selects the path with low delay and high residual bandwidth without, but cannot satisfy the QoS. The MOR algorithm of different services to select suitable paths for different services, but does not consider the link load. When the network load is large, some links may be congested, and some links are relatively idle. However, the MSR-GLB algorithm considers the load of the network when selecting paths for different services and selects links with relatively small traffic demand for data packet transmission.

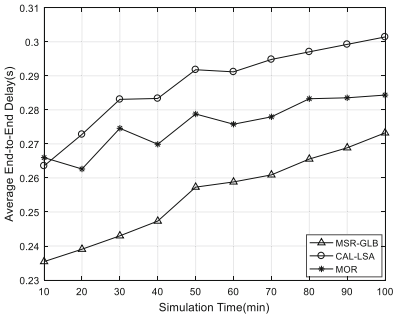

Fig. 4. Average end-to-end delay.

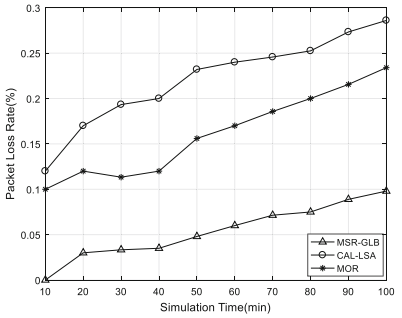

Fig. 5. Packet loss rate.

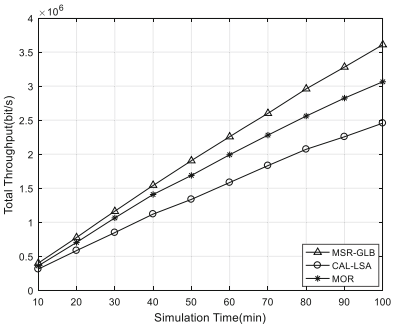

Fig. 6. Throughput.

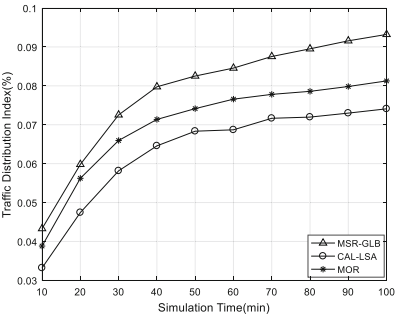

Fig. 7. Traffic distribution index.

6 Conclusion

In this paper, a multi-service routing with guaranteed load balancing (MSR-GLB) algorithm is proposed to meet the differentiated service QoS requirements and balance the network load. Firstly, an Iridium-like LEO network model is constructed with the virtual topology method, and the GLIF is modeled as a function related to the geographic location of the satellite to predict the ISLs traffic load. Secondly, an optimization objective function was formulated based on link QoS information and GLIF in order to describe the multi-service and load routing problems in an Iridium-like LEO satellite network. Thirdly, the state transition rule with QoS information and link GLIF is defined to identify the next-hop node. Meanwhile, the link pheromone updating rule with positive and negative feedback mechanism is presented to improve the search-ability and convergence speed of the MSR-GLB algorithm, and finally, the optimal QoS path of the current service is obtained. Finally, the simulation results show that the MSR-GLB algorithm has obvious advantages in terms of delay, throughput, and packet loss rate and traffic distribution index under the condition of heavy load in the satellite network comparing with MOR and CAL-LSN.

Acknowledgment. This work was jointly supported by the National Natural Science Foundation in China (61601075), the Natural Science Foundation Project of CQUPT (A2019-40).

References

1. Radhakrishnan, R., Edmonson, W.W., Afghah, F., Rodriguez-Osorio, R.M., Pinto, F., Burleigh, S.C.: Survey of inter-satellite communication for small satellite systems: physical layer to network layer view. IEEE Commun. Surv. Tutorials **18**(4), 2442–2473 (2016)
2. Choi, J.P., Chang, S., Chan, V.W.S.: Cross-layer routing and scheduling for onboard processing satellites with phased array antenna. IEEE Trans. Wireless Commun. **16**(1), 180–192 (2017)
3. Werner, M.: A dynamic routing concept for ATM-based satellite personal communication networks. IEEE J. Sel. Areas Commun. **15**(8), 1636–1648 (1997)
4. Mauger, R., Rosenberg, C.: QoS guarantees for multimedia services on a TDMA-based satellite network. IEEE Commun. Mag. **35**(7), 56–65 (1997)
5. Hashimoto, Y., Sarikaya, B.: Design of IP-based routing in a LEO satellite network. In: Third International Workshop on Satellite-based Information Services, pp. 81–88 (1998)
6. Tan, H., Zhu, L.L.: A novel routing algorithm based on virtual topology snapshot in LEO satellite networks. In: IEEE 17th International Conference on Computational Science and Engineering, pp. 357–361 (2014)
7. Liu, Y., Zhu, L.: A suboptimal routing algorithm for massive LEO satellite networks. In: International Symposium on Networks, Computers and Communications (ISNCC), pp. 1–5 (2018)
8. Karapantazis, S., Papapetrou, E., Pavlidou, F.-N.: Multiservice on-demand routing in LEO satellite networks. In: IEEE Transactions on Wireless Communications, vol. 8, no. 1, pp. 107–112 (2009)
9. Jiang, W., Zong, P.: QoS routing algorithm based on traffic classification in LEO satellite networks. In: Eighth International Conference on Wireless and Optical Communications Networks, pp. 1–5 (2011)
10. Jiang, W., Zong, P.: A mew constellation network multi-service QoS routing algorithm. J. Jiangsu Univ. (Nat. Sci. Ed.) **34**(4), 428–434 (2013)
11. Yang, L., Sun, J., Pan, C.: LEO multi-service routing algorithm based on multi-objective decision making. J. Commun. **37**(10), 25–32 (2016)
12. Song, G., Chao, M., Yang, B., Zheng, Y.: TLR: a traffic-light-based intelligent routing strategy for NGEO satellite IP networks. IEEE Trans. Wireless Commun. **13**(6), 3380–3393 (2014)
13. Wang, H., Zhang, Q., Xin, X., Tao, Y., Liu, N.: Cross-layer design and ant-colony optimization based routing algorithm for low earth orbit satellite networks. China Commun. **10**(10), 37–46 (2013)
14. Liu, Z., Li, J., Wang, Y., Li, X., Chen, S.: HGL: a hybrid global-local load balancing routing scheme for the Internet of Things through satellite networks. Int. J. Distrib. Sens. Netw. **13**(3) (2017)
15. Maine, K., Devieux, C., Swan, P.: Overview of IRIDIUM satellite network. In: WESCON 1995, p. 483 (1995)
16. Wood, L., Clerget, A., Andrikopoulos, I., Pavlou, G., Dabbous, W.: IP routing issues in satellite constellation networks. Int. J. Satell. Commun. **19**(1), 69–92 (2001)
17. Rao, Y., et al.: Agent-based multi-service routing for polar-orbit LEO broadband satellite networks. Ad Hoc Netw. **13**(1), 575–597 (2014)
18. Dai, Z.: Research on QoS routing under service classification system. Nanjing University of Posts and Telecommunications (2013)
19. Dorigo, M., Maniezzo, V., Colorni, A.: Ant system: optimization by a colony of cooperating agents. IEEE Trans. Syst. Man Cybern. Part B (Cybern.) **26**(1), 29–41 (1996)

20. Mouhcine, E., Khalifa, M., Mohamed, Y.: Route optimization for school bus scheduling problem based on a distributed ant colony system algorithm. In: 2017 Intelligent Systems and Computer Vision (ISCV), pp. 1–8 (2017)
21. Wen, G., et al.: Cross-layer design based ant colony optimization for routing and wavelength assignment in an optical satellite network. In: 2016 15th International Conference on Optical Communications and Networks (ICOCN), pp. 1–3 (2016)